Piet Hut's
Feb. 05

Plasma Physics for Astrophysics

RUSSELL M. KULSRUD

PRINCETON UNIVERSITY PRESS

PRINCETON AND OXFORD

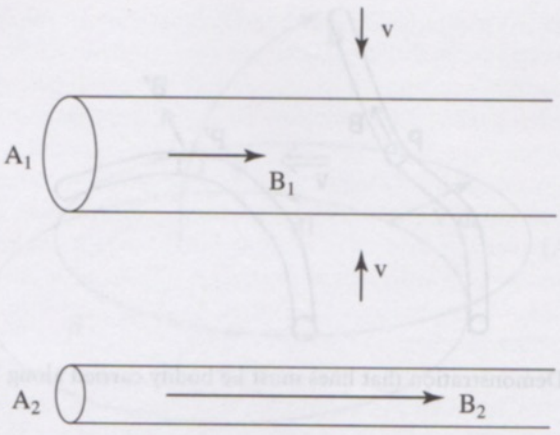

Figure 3.3. Compression perpendicular to B

two different components of the field, the poloidal and toroidal fluxes are respectively frozen.

Our description and proofs of flux freezing are semiquantitative. Later we shall introduce a more analytical description for the change in B (problem 2 and Lundquist's identity, equation 75 in chapter 4. For the moment let us discuss some applications that bring out the importance and usefulness of the flux freezing.

3.3 Applications of Flux Freezing

3.3.1 The Symmetric Cases

We now take up some simple examples of flux freezing. First consider a uniform plasma and a uniform magnetic field, taken in the z direction, and let there be motion of the plasma perpendicular to B that is independent of z as in figure 3.3. Follow a cylinder of cross-sectional area A. Both the mass and the flux in this cylinder are conserved. Therefore, ρA and BA are conserved and we have

$$\frac{B}{\rho} = \text{constant} \tag{26}$$

Next consider motion parallel to B but now dependent on z. In this case the cross-sectional area of a cylinder is preserved so B = constant. This is valid, even though ρ for some plasma of length ℓ changes as $1/\ell$. $\rho\ell$ is constant so $\rho \sim 1/\ell$ and changes. We can say in this case that for such motions,

$$\frac{B}{\rho\ell} = \text{constant} \tag{27}$$

Next consider a uniform isotropic contraction of the plasma toward the origin. The plasma in a sphere of radius r not necessarily at the origin conserves mass and flux so that both ρr^3 and Br^2 are constant and so

$$\frac{B}{\rho^{2/3}} = \text{constant} \tag{28}$$

Collecting these three cases together we have

$$\frac{B}{\rho^n} = \text{constant}$$

$$\begin{aligned} n &= 1 \quad \text{Perpendicular contraction or expansion} \\ n &= 0 \quad \text{Parallel contraction or expansion} \\ n &= \tfrac{2}{3} \quad \text{Isotropic, contraction or expansion} \end{aligned} \tag{29}$$

Thus, in these symmetric cases there exists a simple relation between field strength B and density ρ, but the relation depends on the particular symmetry. Such relations, which are occasionally invoked in astrophysics, must be handled with care.

3.3.2 Stellar Collapse

Now, let us consider some more specific cases. First a collapsing star. Let a star of radius $\approx 10^{11}$ cm collapse to a white dwarf of radius 10^9 cm. If this collapse is isotropic, $B \sim \rho^{2/3}$ and ρ increases by $(10^{11}/10^9)^3 = 10^6$ so the magnetic field increases by $(10^6)^{2/3} = 10^4$. For example, an initial field of 10^2 G increases to 10^6 G. Such fields are frequently observed in white dwarfs and flux freezing makes clear why they should be present.

For a more extreme case consider the isotropic collapse of the same star to a neutron star of radius 10^6 cm and density 10^{15} g/cm^3. The radial collapse of r from 10^{11} to 10^6 means a decrease of r by 10^{-5} and area $\sim r^2$ by 10^{-10}, so the field would be increased by 10^{10}, say from 100 G to 10^{12} G (a typical field for a neutron star).

Let us ask whether flux conservation is a reliable assumption. To check this, let us go to the magnetic field equation with resistivity, equation 18:

$$\frac{\partial \mathbf{B}}{\partial t} = \nabla \times (\mathbf{V} \times \mathbf{B}) + \frac{\eta c}{4\pi} \nabla^2 \mathbf{B}$$

The factor $\eta c/4\pi$, the resistivity of the plasma, is very weakly (logarithmically) dependent on density and is proportional to the electron temperature to the minus three-halves power, $T_e^{-3/2}$ Its value at $T = 10^4$ K is $\approx 10^7$ cm^2/sec, so

$$\frac{\eta c}{4\pi} \approx \frac{0.42 \times 10^7}{T_{\text{eV}}^{3/2}} \text{ cm}^2/\text{sec} \tag{30}$$

where T_{eV} is the temperature in electron volts. Its dimensions are clear from equation 18. If we estimate $\nabla^2 \sim 1/L^2$, where L is the scale length over

which B varies, then the last term is of order B/T_{decay}, where (without the 0.42 factor)

$$T_{\text{decay}} \approx 10^{-7} T_{\text{eV}}^{3/2} L^2 \text{sec} \tag{31}$$

For the white dwarf with $T_{\text{eV}} = 10^2$ (10^6 K) and $L \sim R \sim 10^9$ cm we find $T_{\text{decay}} \approx 10^{-7+3}(10^9)^2 = 10^{14}$sec. The time-derivative term in equation 18 is B/t, where t is the timescale during which a star collapses to reach the white dwarf stage. Thus, the resistive term is negligible compared to the time derivative term if

$$t \ll T_{\text{decay}} = \frac{L^2}{\eta c/4\pi} \tag{32}$$

(Cowling 1976).

Flux freezing results from balancing the $\partial B/\partial t$ and the $\nabla \times (V \times B)$ term. If t is shorter than 10^{14} sec $= 3 \times 10^6$ years, then the resistivity term is negligible, these other two terms must balance, and we can safely assume flux freezing.

Our discussion has been very rough. η varies with T_{eV} and it and L^2 clearly change by large factors as the star collapses, so the effective decay time T_{decay} is probably larger than the above estimate. Also, the later stages of collapse occur faster. Since the total collapse term is probably shorter than 10^{14} sec, our criteria for flux freezing is even more strongly satisfied.

A similar calculation for increase in the magnetic field during the collapse of a neutron star performed at its smallest radius with $T_{\text{eV}} \gg 10^4_{\text{eV}}$ $L = 10^6$ cm leads to a decay time of $T_{\text{decay}} > 10^{6-7+12} \approx 10^{11}$ sec. Neutron star collapse occurs on a timescale of a few seconds, so from this calculation flux freezing is also well satisfied in this case.

Let us turn to an example where flux freezing, at least in it simplest form, definitely cannot hold. This example concerns the initial formation of a star. Again, for simplicity, assume that the collapse is isotropic. Let the protostar start with a density of 1 atom/cm^3 and collapse to a uniform sphere with a density of 1 g/cm^3 corresponding to $\approx 10^{24}$ atoms/cm^3. B increases by $(10^{24})^{2/3} = 10^{16}$. Starting with a field of 3×10^{-6} G, characteristic of the interstellar field, its final value would be 3×10^{10} G. Such a magnetic field has a magnetic pressure $B^2/8\pi = 4 \times 10^{19}$ergs/cm^3. Compare this with the internal pressure of a normal star, $nT_{\text{eV}} \approx 10^{24-10} \approx 10^{14}$ ergs/cm. (Here and in the rest of this book we include the Boltzmann constant intrinsically in the temperature, although when we refer to the temperature we continue to mean its value in units of electron volts. This is convenient and never seems to cause a problem.)

We see that such a field could not be present in stars. In fact, such a field would be strong enough to resist gravitational collapse altogether. Also, for a typical star, $T = 10^2$ eV, $L = 10^{11}$ cm, and $T_{\text{decay}} \approx 10^{18}$ sec. Because this is longer than the Hubble time, flux freezing should be valid.

To understand what must happen, we have to appreciate that before the star can form, the interstellar matter must have a very low degree of ionization, and the neutrals and the ionized component need not move together. In fact, the magnetic $\mathbf{j} \times \mathbf{B}$ forces act only on the ionized component. The ionized component cannot collapse at all because of this strong force. The neutral component can collapse, but its collapse is limited by the collision of the neutrals with the stationary ions. The balance of forces give

$$n_0 n_i m_H V_r \langle \sigma v \rangle = n_o m_H g = n_0 m_H \left(\frac{GM}{R^2} \right) \tag{33}$$

where m_H is the mass of atomic hydrogen, n_i is the ion density, V_r is the radial velocity of the collapse, $n_i \langle \sigma v \rangle$ is the collision rate, g is the (inward) gravitational force, and n_0 is the neutral density. $\langle \sigma v \rangle$ is of appreciable size, but when n_i becomes very small, V_r can become large enough to lead to collapse of a star in a reasonable time.

Note that the same forces on the neutrals that occur in this equation are also exerted on the ionized component, since the total collisional forces are equal (and opposite), by momentum conservation of each collision. Since the collisional force on the ions is balanced mostly by the Lorentz force, the Lorentz force $\mathbf{j} \times \mathbf{B}$ must balance the right-hand side. Since any appreciable distortion of the field leads to a Lorentz force much larger then the gravitational force on the neutrals, the distortion must be negligible.

To summarize: During collapse, the magnetic field remains frozen in the ions that are held essentially motionless by the large Lorentz force. The neutrals collapse moving through the ions at a velocity such that the collisional force with the ions just balances the gravitational collapse force. This process of stellar formation is called ambipolar diffusion (Elmegreen 1985).

3.3.3 The Solar Wind and the Magnetosphere

Next we consider the solar wind and its interaction with the earth's magnetic field. The solar wind cannot enter the region of the earth's field because to do so would violate flux freezing. The solar wind is "frozen off of" the earth's magnetic field lines. Alternatively, if the plasma did enter the field we could consider it frozen onto the earth's field lines. Turning time around the plasma could not leave and return to the sun. Note that equation 17, from which flux freezing derives, is time reversible.

Thus, insofar as flux freezing holds, the solar wind plasma cannot enter the earth's magnetic field. When it encounters the earth it must flow around on either side of the earth's field. This deflection of the solar wind requires a considerable force. This leads to a compression of the earth's magnetic field into a closed cavity, called the magnetosphere. By balancing the force resulting from the compression of the earth's field with the pressure exerted by the solar wind on it we find that the size of the earth's magnetic cavity is between 8 and 10 earth radii. Indeed, from measurements of this cavity

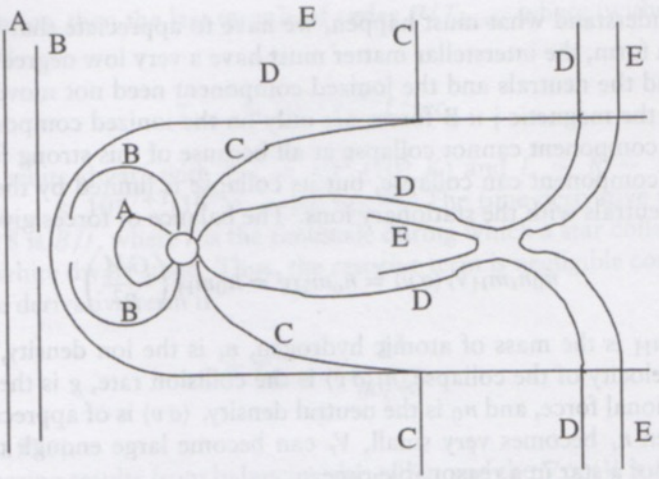

Figure 3.4. The reconnected lines at four different positions, A, B, C, D, E

by satellites, we find that this is its approximate size in the direction toward the sun, and also that as the speed and density of the solar wind change, the radius of the cavity varies between these two scales. It is smaller when the solar wind is more intense.

On the downstream side of the earth, away from the sun, the picture is very different from what would be expected from perfect flux freezing. With flux freezing, we would expect that the shape would be a teardrop, with the cavity ending in a point where the solar wind from the different transverse sides of the cavity come together. Instead, the earth's field fills a long, cylindrical cavity extending many hundreds of earth radii downstream. The inside of this cylinder is called the earth's magnetotail, perhaps in analogy with a comet tail.

The explanation for this is due to Dungey (1961). He postulated that when the magnetic lines carried by the solar wind come in contact with the earth's magnetic lines of force, not all of the solar wind's lines pass smoothly around the earth. He supposed that 5 to 10 percent of the solar wind's magnetic lines break. Simultaneously, an equal number of the earth's magnetic lines break. The broken lines of different types join, or reconnect, the earth's broken lines connecting to the solar wind's broken lines (Hughes 1995). The result of this breaking and reconnecting can be visualized from figure 3.4, where the positions of five different pairs of lines, A, B, C, D, and E, at a given time are shown. If the situation is in a steady state, we can visualize these five positions as indicating the change in time of a single pair of lines.

Start with pair A. The left line of the pair is in the solar wind and is approaching the earth with the solar wind velocity. The right line of the pair is connected to the earth. It will move to touch the solar wind. The pair will then occupy the position of the pair B. The two lines break and the northern

This requires opposite field directions in the pair

parts of the lines in the pair will reconnect, as will the southern parts. The two parts of the pair are now each connected to the earth and embedded in the solar wind. The solar wind parts of the lines continue to move with the solar wind velocity.

At a later time the lines are at position C, where the solar wind part of the line is being carried rapidly downstream, pulling the earth's part of the line far downstream. The stretched part of our line and other such lines form the magnetotail of the earth. This stretching continues until a second breaking of the line occurs at the position of the pair D. The solar wind line again reattaches to its original part at position E.

Subsequently, the restored solar wind is swept downstream without further disturbance. However, after reconnection the earth's part of the line is greatly stretched and is expected to snap back to the earth, delivering the considerable energy it has obtained from the energy of the solar wind velocity to the inner part of the earth's magnetosphere. This can generally lead to a large disturbance, which is often credited with being responsible for magnetic substorms and aurora.

This crude picture seems to correspond remarkably well to what is observed. That breaking of the flux-freezing condition occurs here is not so surprising when it is appreciated that the contact surface between the solar wind and the magnetosphere is very thin and, because the magnetic field is quite different across it, the current density is very large. Thus, the ηj term in Ohm's law, equation (10), or, alternatively, the diffusion term $(\eta c/4\pi)\nabla^2 B$ in the magnetic differential equation 18 need no longer be negligible. However, as shown in chapter 14, a closer look at the *reconnection* event that occurs in the narrow layer shows that only a tiny number of lines should reconnect on the basis of the resistive ideal equations, that is to say, only a much smaller fraction than 5–10 percent of the lines reconnect. The resolution of this discrepancy is a subject of great current interest. The subject of the reconnection of lines over this layer is called magnetic reconnection and is very important. We devote chapter 14 entirely to magnetic reconnection.

The conditions on the surface of the magnetosphere are so extreme that even the resistive ideal equations cannot adequately describe them. Much microscopic physics comes in. Shocks and intense microscopic waves appear that may enhance the resistivity. It is probable that these phenomena are responsible for the substantial amount of reconnection that is actually observed. It is interesting that after a line reconnects it stays reconnected for a good portion of a day before it separates back to its previous state. During this time it can be drawn downstream about 1000 earth radii.

In the Dungey picture the concept of flux freezing is valid everywhere except in a tiny region on the sunward side of the surface of the magnetosphere, and at one point far down the magnetotail. But these tiny regions change the topology of the lines and this has a profound effect in changing the whole picture of the solar wind interaction with the magnetosphere, producing the magnetotail, the magnetic storms, and the aurora near the earth's polar caps.

Another remarkable phenomenon that can be easily understood in terms of flux freezing is the spiral structure of the lines of force in the solar wind (Parker 1963). Beyond about ten solar radii the solar wind velocity is found to be nearly radial. Let us imagine a blob of solar wind plasma with azimuthal angle $\theta = 0$ near the sun that moves out radially, starting at time $t = 0$. If the sun were not rotating, the blob would draw the line of force out of the sun in the strictly radial direction. But because of rotation, the position of the next blob, which was at $\theta = 0$ at $t = 0$, is at $\theta = \Omega t$ at time t. If these two blobs were on the same line of force, the line must connect the first blob at $\theta = 0$, $r_1 = V_0 t_1$ with the second blob at $r = 0$, $\theta_2 = \Omega t_1 = (r_1/V_0)\Omega$. It is easily seen that at later times the points that are connected lie along the curve

$$\theta = r\frac{\Omega}{V} \quad \text{or} \quad r = \frac{V\theta}{\Omega} \tag{34}$$

the equation of an Archimedian spiral. The angle α this curve makes with the azimuthal direction satisfies

$$\tan\alpha = \frac{dr}{rd\theta} = \frac{V}{\Omega r} \tag{35}$$

with $\Omega = 3 \times 10^{-6}$. At the earth $r = 1$ a.u. $= 1.5 \times 10^{13}$ cm and taking $V = 3.5 \times 10^7$ cm/sec, we find that $\alpha \approx 45°$ at the earth, which is close to the observed angle. Note that for large r, $\alpha \sim 1/r$ and the spiral becomes flatter at large distances, also in agreement with observations.

3.3.4 Stellar Formation and the Angular Momentum Problem

Let us return to star formation for another important example where flux freezing plays a crucial role, We earlier showed how magnetic fields inhibit star formation since the interstellar magnetic field is too strong to be drawn into the newly forming protostar. In exactly the same way, angular momentum inhibits star formation. Conservation of angular momentum Ωr^2 means that as the star collapses its angular velocity increases. In fact, we have $\Omega \sim r^{-2} = \rho^{2/3}$. Thus, if ρ increases from $\rho = 10^{-24}$ g/cm^3 to $\rho = 1$ g/cm^3, Ω increases by $(10^{24})^{2/3} \approx 10^{16}$. The initial blob of plasma has at least the angular velocity of the galaxy $\Omega \approx 2\pi/(200 \times 10^8 \text{ yr}) = 10^{-15}$ radians/sec, so the collapsed star would have $\Omega = 10\,\text{sec}^{-1}$, much too fast too allow the star to collapse.

This angular momentum barrier can be removed by the interstellar field (Elmegreen 1985). The field lines in the collapsing star are also connected to the neighboring part of the interstellar medium not directly involved in the collapse. See figure 3.5, where B is parallel to Ω. As the star collapses the lines becomes twisted about the rotational axis Ω.

The twisted field lines passing through both the star and the interstellar medium have a current j that leads to magnetic forces that exert a backward torque on the star and a forward torque in the cylindrical column not

Figure 3.5. The transfer of angular momentum from a rotating protostar to the interstellar medium by the interstellar field

included in the sphere. The result is that the angular momentum of the collapsing star is shared with a piece of the column. The length of the column that is forced to corotate is $v_A t$, since the twist in the line is actually an Alfven wave propagating up the interstellar field (see problem 4). Assuming initially that the density of the column and the sphere are the same, we see that the angular velocity Ω of the protostar decreases as

$$\Omega = \frac{\Omega_0}{1 + v_A t / R_0} \tag{36}$$

where R_0 and Ω_0 are the initial values of the protostellar radius and angular velocity, and the Alfven speed is $v_A = B/\sqrt{4\pi\rho}$. This decrease continues until the lines starts to slip, by ambipolar diffusion, through the neutral component of the sphere. Generally, a large enough angular momentum is removed to allow collapse. (It is now appreciated that in the later stages of collapse further angular momentum is removed by formation of a disk and the existence of anomalous viscosity in the disk.) The magnetic field has a twofold role in the stellar formation. First it removes a sizable fraction of angular momentum, helping to break through the angular momentum barrier. Then through its radial stress it resists further collapse until ambipolar slippage occurs.

3.3.5 Magnetic Fields in Turbulence

Now let us consider a turbulent flow of a weakly magnetized infinitely conducting plasma. Let us follow a short piece of a magnetic tube of force of cross-sectional area A and of length ℓ.

By flux conservation,

$$\Phi = BA = \text{constant} \tag{37}$$

3.6 The Validity of the MHD Equations

In the preceding sections we have considered general properties of MHD plasmas. Remember that this MHD description of a plasma is valid only if there are sufficient collisions to give it fluid properties. Let us estimate the required collision rate. For example, we regard a given cube of plasma with its mass energy and momentum as a unit. If too many particles leave the cube, it will not preserve its unity and the equations for it will not be valid.

Take such a cube and let it have a scale L comparable to or a somewhat smaller than the scale of variation of the plasma quantities ρ, p, and V. If particles leak out of this cube in a time short compared to T, the time for the plasma quantities to change, then we cannot regard the cube as a unit of plasma, and the MHD equations fail. Let the typical mean free path for the plasma particles be λ, their thermal velocity be v_T, their collision rate be ν, and their collision time be $\tau = 1/\nu$. Then in a time T a particular plasma particle will random walk a distance ℓ with

$$\ell^2 = \frac{T}{\tau}\lambda^2 \approx T v_T \lambda \tag{49}$$

since it will make T/τ collisions, and between each collision it will move a distance λ in a random direction with the direction of the steps uncorrelated. (More formally, $\ell^2 = \langle(\Sigma x_i)^2\rangle$ and $\langle x_i^2\rangle = \lambda^2$, $\langle x_i x_j\rangle = 0$, where angle brackets denote averages. We use the fact that $\lambda = v_T\tau$.)

Thus, our treatment of the plasma as a fluid is justified if $\ell^2 \ll L^2$ or

$$v_T\lambda \ll \frac{L^2}{T} \tag{50}$$

This condition is satisfied if

$$\nu \ll \frac{1}{T} \quad \text{and} \quad \lambda \ll L \tag{51}$$

since $v_T\lambda = \lambda^2\nu$.

There are further conditions that must be satisfied, such as a sufficiently small thermal conductivity that entropy is conserved and a small enough viscosity that the pressure remains isotropic. These conditions are discussed in full detail in chapter 8. For the moment let us restrict ourselves to the criteria of equation 51 for judging the validity of the MHD equations.

To apply these rough criteria, we give the prescription for a qualitative determination of ν and λ. For these quantities we need an estimate of the appropriate Coulomb collision cross section, which is the effective cross section for scattering of a particle through 90°. (This will be pursued in more detail in chapter 8.) Electrons scatter off of both ions and electrons and the cross section is of order

$$\sigma \approx \frac{10^{-12}}{T_{\text{eV}}^2}\text{cm}^2 \tag{52}$$

where T_{eV} is the electron temperature in electron volts. A temperature of one electron volt is equivalent to a temperature of 10^4 K. Ions primarily scatter off only ions and not off electrons. Their cross section is given by equation (52), with the ion temperature instead of the electron temperature. In addition, we might multiply it by a factor of order one-half because there are only half as many collisions. (But see the last section of chapter 8.)

For equal temperatures, the mean free path is roughly the same for electrons and ions and is

$$\lambda = \frac{1}{n\sigma} \tag{53}$$

where n is either the ion or electron density. (They are the about same for a hydrogenic plasma.) The collision rate is

$$\nu = \frac{v_T}{\lambda} \tag{54}$$

where v_T is the thermal velocity of the appropriate species. Because for the same temperature the thermal speed is larger for electrons than for ions by a factor of 40 (the square root of the mass ratio), ν is larger for electrons than for ions by the same factor. At 1 eV $\approx 10^4$ K, $v_T \approx 7 \times 10^7$ cm/sec for electrons, and $v_T \approx 1.5 \times 10^6$ cm/sec for ions.

If the plasma is partially ionized, then there will also be collisions with neutrals. However, the atomic scattering cross section is the gas atomic cross section of about 10^{-16} cm^2. Because this is much smaller than the Coulomb cross section at 1 eV, collision rates with neutrals are much smaller than collision rates with other ions and can generally be neglected. At higher temperatures, when the Coulomb cross section is smaller, the plasma will be fully ionized, while at lower temperatures the Coulomb cross section is even larger. Thus, as a general rule, electrons and ions are tightly coupled compared to the coupling of electrons with neutrals.

3.7 Pulsar Magnetospheres

The plasmas we have discussed so far have all consisted of ions and electrons with nearly equal densities. As remarked in the introduction, the relative balance between these densities is of order $(\lambda_D/L)^2$. However, there is one noteworthy example, the magnetosphere around a rotating neutron star or pulsar, where charges of only one sign occur. A neutron star is a compact star of solar mass with a radius of 10^6 cm, so its surface gravitational acceleration is 10^{14} cm^2/sec and the ion scale height for a temperature of 100 eV is about 1 cm. Thus, it was at first supposed that the density in its atmosphere must be near that of a vacuum, $\sim 10^{-10^6}$ cm^{-3}.

However, it was pointed out by Goldreich and Julian in 1969 that a magnetized neutron star rotating with an angular velocity ω must have a very strong electric field. For a one-second-period pulsar with a magnetic field